

CONF-900312--1

1263-09

### Soft X-Ray Resist Characterization: Studies with a Laser Plasma X-Ray Source

Glenn D. Kubiak and Duane A. Outka  
Sandia National Laboratories  
Livermore, CA 94551-0969

John M. Zeigler<sup>s</sup>  
Sandia National Laboratories  
Albuquerque, NM 87185

SAND--90-1534C  
DE90 013493

#### ABSTRACT

Little work has been performed to characterize the exposure sensitivity, contrast, and tone of candidate resists for photon energies between 100-300 eV, the range in which projection soft x-ray lithography will be developed. We report here the characterization of near-edge x-ray absorption fine structure (NEXAFS) spectra, exposure sensitivity, contrast, and post-exposure processing of selected polysilane resists at photon energies close to the Si L<sub>2,3</sub> absorption edge (100 eV). We find absorption resonance features in the NEXAFS spectra which we assign to excitation into Si-Si and Si-C  $\sigma^*$  orbitals. Using monochromatized XUV exposures on the Si-Si  $\sigma^*$  resonance at 105 eV, followed by solvent dissolution development, we have measured the exposure sensitivity curves of these resists. We find sensitivities in the range of 600-3000 mJ/cm<sup>2</sup> and contrasts in the range from 0.5 - 1.4, depending on the polysilane side chain. We have also performed exposure sensitivity measurements at 92 eV, below the edge. Sensitivity decreases slightly compared to 105 eV exposures and the saturation depth and contrast both increase, as expected. We find also that exposing resist films to oxygen after XUV exposure, but before development, increases the sensitivity markedly.

#### 1. INTRODUCTION

A recent development in lithographic imaging is projection soft x-ray lithography.<sup>1-3</sup> This method employs highly reflective ( $R \sim .5$ ) multilayer-coated optics in near-normal incidence to project a demagnified image of the object plane onto a photoresist. The optimum wavelengths for such a scheme are thought to be near 125 Å and 55 Å, respectively. These correspond to the wavelength regions in which: a) peak reflectances are achieved with today's synthetic multilayer mirrors, and b) a resolution of at least 0.2  $\mu$ m and a depth of focus of  $\pm 1 \mu$ m can be simultaneously achieved in a projection system having an N.A. of  $\leq 0.1$ .

One of the many problems relevant to this technology concerns the resists; most materials absorb too strongly to allow single-layer resist schemes to be implemented at a resolution equal to that imposed by the diffraction limit of the projection optics. In fact, the tentative optima quoted above have been determined with little regard to all but organic resists<sup>2</sup>. This is not surprising since little is known regarding the performance of candidate resist materials exposed in the soft x-ray and extreme ultraviolet (XUV) regions. Until a wide variety of resists are characterized in these regions, the identification of the true wavelength optima will remain an open question. In particular, Si-containing resists may perform well in the region near 125 Å (99 eV).

We report here an extension of earlier work<sup>4</sup> on the characterization of the soft x-ray absorption spectra, exposure sensitivity, and contrast of polysilane resists exposed at the Si L<sub>2,3</sub> absorption edge near 100 eV. We have used a monochromatized laser plasma source (LPS) to perform all measurements. Near edge x-ray absorption fine structure (NEXAFS) spectra reveal the presence of absorption resonances associated with excitation from Si 2p electronic levels into Si-Si  $\sigma^*$  and Si-C  $\sigma^*$  orbitals, respectively. In an attempt to maximize chain scission during XUV exposures, spin-cast polysilane films have been exposed at the peak of the Si-Si  $\sigma^*$  resonance, 118 Å (105 eV). The

DISTRIBUTION OF THIS DOCUMENT IS UNLIMITED

MASTER *mg*

Kubiak

## DISCLAIMER

**This report was prepared as an account of work sponsored by an agency of the United States Government. Neither the United States Government nor any agency Thereof, nor any of their employees, makes any warranty, express or implied, or assumes any legal liability or responsibility for the accuracy, completeness, or usefulness of any information, apparatus, product, or process disclosed, or represents that its use would not infringe privately owned rights. Reference herein to any specific commercial product, process, or service by trade name, trademark, manufacturer, or otherwise does not necessarily constitute or imply its endorsement, recommendation, or favoring by the United States Government or any agency thereof. The views and opinions of authors expressed herein do not necessarily state or reflect those of the United States Government or any agency thereof.**

## **DISCLAIMER**

**Portions of this document may be illegible in electronic image products. Images are produced from the best available original document.**

**THIS PAGE  
WAS INTENTIONALLY  
LEFT BLANK**



25 ns) output of the LPS. Exposure sensitivities were calibrated before or after each exposure sequence using a diamond photo-conductive detector which had previously been calibrated at a synchrotron to have a sensitivity of  $5 \times 10^{-4}$  amps/Watt.<sup>10</sup> Sample exposures were made on a small region of the resist layer for a specified number of laser pulses in vacuum, the sample was then translated to expose a virgin region and the procedure repeated. After exposure, the samples were developed in 20% tetrahydrofuran (THF) in isopropanol (IPA) for 2-4 minutes at room temperature. As has been noted previously for deep-UV exposures performed in air<sup>5</sup>, increasing concentrations of THF improve the apparent sensitivity of PCMDS but degrade resolution. We find this effect to be even more pronounced for x-ray exposures performed *in vacuo*. Film thickness measurements were performed with a profilometer (Tencor Inst. Alpha-Step 200) scanned through the center of the  $\sim 300 \mu\text{m}$  wide spot formed by the focused x-ray beam.

## 2.2 Laser Plasma Source for Spectroscopy and Resist Exposures

A laser-produced plasma of XUV radiation was used for spectroscopic analysis near the Si  $L_{2,3}$  absorption edge and to expose resists with calibrated doses of monochromatized radiation at wavelengths corresponding to specific spectroscopic absorption features. The LPS is diagrammed schematically in Fig. 2. Briefly, it consists of a three-stage excimer laser system comprised of an unstable resonator, followed by two amplification stages. The laser operates at 249 nm (KrF), producing 1.5 Joule, 25-30 ns-long pulses at 100 Hz repetition rate. The laser is focused onto a gold-coated stainless steel drum which rotates to expose a fresh gold surface to the incident laser every 5-10 laser pulses. The plasma which forms at the focus has a diameter of  $\sim 200\text{-}300 \mu\text{m}$ , as determined with a carbon-filtered x-ray pinhole camera. A slit-less high-throughput monochromator<sup>11</sup> collects a fan of plasma radiation and focuses it stigmatically onto the exit slit. The net collection efficiency, including the reflection efficiencies of the pre-mirror and grating, is  $10^{-4}$ . The measured focal diameter is  $300 \mu\text{m}$ . The target and monochromator are housed in vacuum chambers having nominal base pressures of  $5 \times 10^{-9}$  Torr.

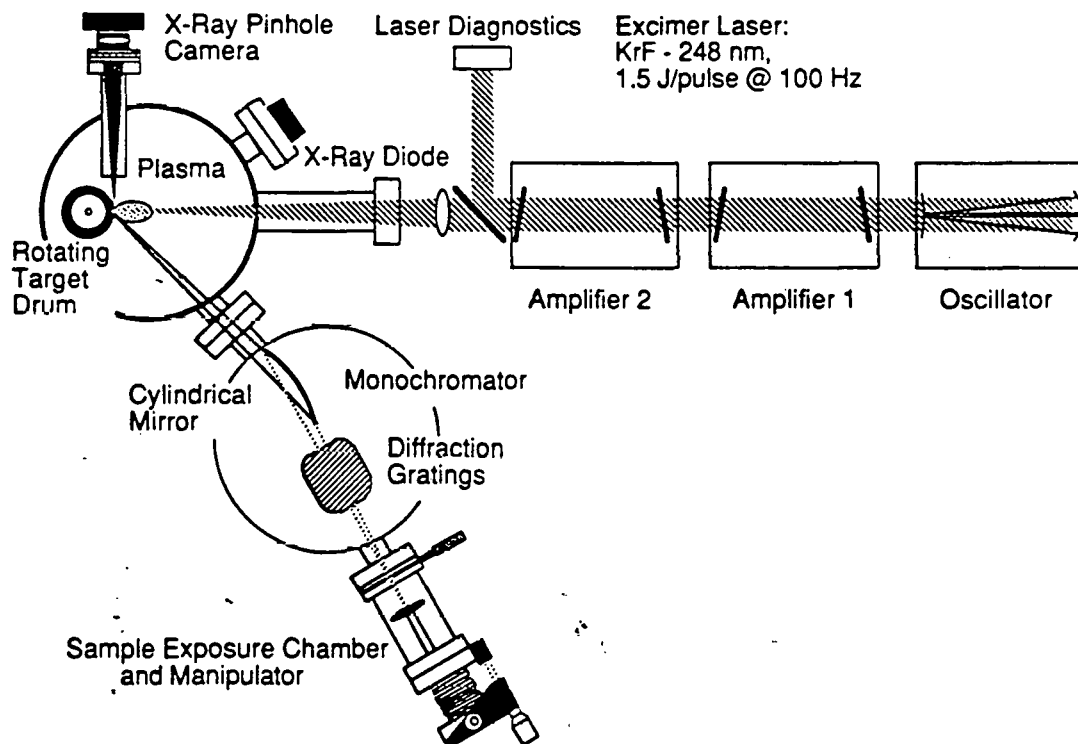


Figure 2. Schematic diagram of the laser plasma source.

**THIS PAGE  
WAS INTENTIONALLY  
LEFT BLANK**

Figure 4 shows unpolarized NEXAFS spectra of *unexposed* CMDM, PMS, CMTMS, and PMTMS in the region of the Si L<sub>2,3</sub> edge. All spectra share the basic attributes of sharp peaks near the edge and broad, structureless features 20-35 eV above the edge. These latter features are known to be sensitive to the geometry of the local molecular environment surrounding Si. They are not relevant to the present study and will not be discussed further. The assignments near the edge are based on the results of quantum chemical calculations (discussed below) performed for model disilanes with various substituents. CMDM and CMTMS both show a poorly resolved shoulder at 103 eV. We assign this resonance to excitations into antibonding Si-C  $\sigma^*$  orbitals associated with the alkyl side groups. The peak observed at 104.5 eV in CMDM and CMTMS is assigned to Si-Si  $\sigma^*$  resonances involving excitation of states antibonding with respect to the polymer backbone. We assign the resolved shoulder at 103 eV in PMS and the poorly resolved shoulder in PMTMS to overlapping Si-Si  $\sigma^*$  and Si-C(methyl)  $\sigma^*$  resonances. The Si-Si  $\sigma^*$  feature is downshifted with respect to the all-alkyl substituted materials presumably because of the electron withdrawing character of the phenyl substituent when bound to Si. The broad feature seen near 106 eV in PMS is assigned to a Si-C(phenyl)  $\sigma^*$  resonance.

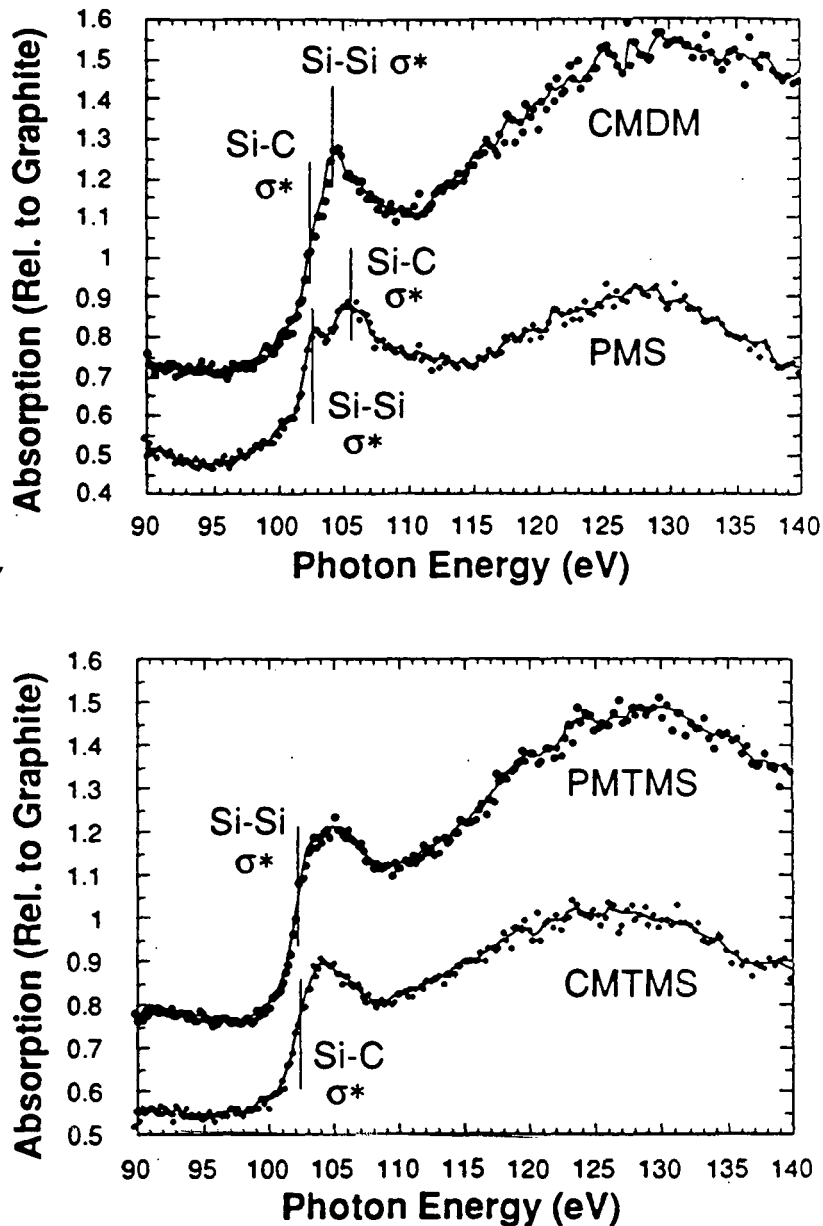


Figure 4 NEXAFS spectra of four polysilane films recorded near the Si L<sub>2,3</sub> edge.

The assignments proposed are based in part on quantum chemical calculations of the electronic structure of model disilanes<sup>13</sup>. While these calculations do not attempt to consider the full polymer, we believe the calculated changes in electronic energy levels as a function of side group functionality are qualitatively correct for assigning experimental spectra. These calculations predict that Si-Si  $\sigma^*$  virtual levels will lie 1.4 eV higher in energy than Si-C  $\sigma^*$  levels in 1,2 dimethyl disilane. Experimentally, the two features seen in the purely alkyl-substituted CMDM are split by 1.5 eV. Calculations performed for

THIS PAGE  
WAS INTENTIONALLY  
LEFT BLANK



addition, the absorption intensity in the region of the Si-O resonances has increased slightly. It appears that oxidation occurs for CMDM after *in vacuo* XUV exposure, suggesting that films handled in air after such exposure are not completely stable. We are unable to determine from the NEXAFS data alone what metastable (with respect to oxidation) species are formed as a result of irradiation, however.

### 3.2 Soft X-ray Exposure Sensitivity

Sensitivity curves at exposure wavelengths near the Si  $L_{2,3}$  absorption edge were obtained for CMDM, CMTMS, and PMTMS. Data will be presented only for the first two of these materials, however. We express sensitivity as that dose,  $D_{Sat}$ , which removes film to the saturation depth. The saturation depth is determined by the film absorbance at a given wavelength and is approximately 0.2  $\mu\text{m}$  at 105 eV for the polysilanes studied. Fig. 7 shows the sensitivity curves of two CMDM samples following exposure at 105 eV. One sample was developed in THF/IPA within minutes of its removal from vacuum and the other was cured in air for approximately 10 days before development. The film developed shortly after exposure (solid line, diamonds in Fig. 7) exhibits  $D_{Sat} = 3000 \text{ mJ/cm}^2$  and  $\gamma = 1.4$ . In comparison,  $D_{Sat}$  of the film cured in air (dashed line, circles in Fig. 7) is reduced to  $1000 \text{ mJ/cm}^2$  although  $\gamma$  is reduced to 0.5. As previously noted<sup>4</sup>, these results are consistent with observations<sup>8</sup> that silylenes and small chain fragments are formed during *in vacuo* chain scission. Silylenes are known to be unstable with respect to oxidation and would thus be expected to form from the irradiated polysilane over time as oxygen diffused into the film. The NEXAFS data in Fig. 6 supports this idea; the Si-Si  $\sigma^*$  resonance intensity decreases after *in vacuo* production of silylenes and other species and these are subsequently oxidized, yielding Si-O resonances.

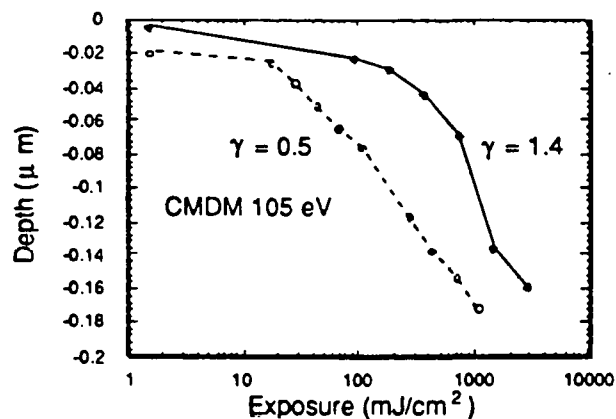


Figure 7. Exposure sensitivity curves for uncured (diamonds) and air-cured (open circles) CMDM recorded following monochromatized exposures at 105 eV.

CMTMS was the most extensively studied of the polysilanes chosen for the present investigation. Fig. 8 shows exposure sensitivity curves for this resist at 105 eV; the most striking aspect of these results is that the tone of CMTMS reverses after a threshold dose of  $\sim 600 \text{ mJ/cm}^2$ . Fig. 8 also demonstrates the effect of development time on  $D_{Sat}$  and  $\gamma$ . The films in panels a) and b) were developed in 20 % THF/IPA for a total of 2 min. and 4 min., respectively. The effect of increased development time is to decrease  $\gamma$  from 1.4 to 1.0. Note that CMTMS is  $\sim 5$  times more sensitive than CMDM in the region of exposure dose where it exhibits positive tone. Monochromatized exposures were also performed at 92 eV in an attempt to increase the saturation absorption depth and  $\gamma$ . The results are illustrated in Fig. 9 and show that the saturation depth,  $D_{Sat}$ , and  $\gamma$  have increased to values of 0.25  $\mu\text{m}$ ,  $1000 \text{ mJ/cm}^2$ , and  $\sim 1.7$ , respectively. Tone reversal is also observed at this wavelength.

**THIS PAGE  
WAS INTENTIONALLY  
LEFT BLANK**

situation, the direct photochemistry which occurs at the photoabsorption site can be masked by the indirect, electron-induced chemistry which occurs subsequently. It may therefore be of little consequence whether the exposure wavelength corresponds to a specific molecular resonance, although generalizing this result must await more extensive resist characterization in the XUV.

The exposure sensitivity measurements of CMDM and CMTMS exhibit moderate contrast and low sensitivity. The contrast observed for XUV exposures in vacuum is far less than the value of 3.1 observed under deep-UV exposures<sup>5</sup>. Low contrast has also been observed in CMDM for 20 keV electron beam exposures<sup>5</sup> and has been attributed to an increase in crosslinking relative to chain scission. Facile crosslinking would also explain the tone reversal seen at high exposures for CMTMS. Of the two materials which were studied at high exposures (CMDM and CMTMS), it is interesting to note that tone reversal is observed only in CMTMS. The reason for this has not been investigated in detail but we speculate that Si-Si bond cleavage in CMTMS yields a mobile  $\cdot\text{Si}(\text{CH}_3)_3$  radical which allows for more efficient crosslinking than occurs after Si-Si bond cleavage on the polymer backbone itself. The diradical formed in the latter process is sterically hindered and may rebond with a high probability, preventing crosslinking. In contrast, photoabsorption in CMTMS may yield the diradical,  $-\text{Si}-\text{Si}^{\cdot}-\text{Si}-$  and  $\cdot\text{Si}(\text{CH}_3)_3$ . The latter species may move away from its main chain parent, leaving it to bond to an adjacent molecule with high probability.

The values of  $D_{\text{Sat}}$  observed for CMDM, CMTMS, and PMTMS are a reflection of the photochemistry occurring in each of these polymers following absorption. While we have not yet determined the chain scission and crosslinking quantum yields resulting from XUV exposures, the relative values of  $D_{\text{Sat}}$  can be rationalized on the basis of the known UV photochemistry. It is known<sup>15</sup> that both CMTMS and PMTMS exhibit low fluorescence quantum yield in solution upon excitation near 300 nm. Low quantum yields imply high photochemical sensitivity for the trimethylsilyl substituted polymers, a fact which has been attributed to increased intersystem crossing rates into the photochemically active triplet state. To the extent that the state excited during UV absorption, as well as its subsequent decay, are identical to the situation occurring upon XUV absorption, the silyl-substituted polymers would be expected to be more sensitive photochemically than their purely alkylated cousins. PMTMS, having a  $D_{\text{Sat}}$  approximately equal to that of CMDM, appears to deviate from this trend. It is likely that PMTMS exhibits lower sensitivity than CMTMS due to the presence of the phenyl substituent. Phenyl substituents are known to sharply reduce solid state photochemical sensitivity in the polysilanes<sup>8,16,17</sup> because of strong mixing between  $\sigma$  and  $\pi$  states<sup>18</sup>.

### 3.3 Conclusions

In summary, the photoabsorption and soft x-ray lithographic exposure sensitivity properties of selected polysilanes have been investigated at photon energies near the Si  $L_{2,3}$  absorption edge. The x-ray absorption spectra of polysilane homo- and co-polymers reveal absorption resonances associated with promotion into Si-Si  $\sigma^*$  and Si-C  $\sigma^*$  orbitals. NEXAFS spectra show an attenuation of the Si-Si  $\sigma^*$  resonance upon UV exposure in air and also upon XUV exposure in vacuum followed by oxidation at an  $\text{O}_2$  pressure of 2 atm. These spectra also reveal Si-O  $\sigma^*$  features, consistent with the formation of siloxanes and other oxidation products. Exposure sensitivity curves have been recorded with monochromatized 105 eV radiation, corresponding to the peak of the Si-Si  $\sigma^*$  absorption feature. Sensitivities are low, ranging from 600 - 3000 mJ/cm<sup>2</sup>, with exposure contrasts in the range from 0.5 - 1.4. Sensitivity measurements have also been recorded at 92 eV, below the  $L_{2,3}$  edge, to assess possible changes in resist photochemistry. Results at 92 eV and 105 eV were not significantly different, demonstrating that the specific route of photoexcitation does not play a large role in determining the lithographic properties of these resists. For exposures in the region from 90-110 eV we conclude that polysilanes would be useful only in surface-imaging, bilayer resist schemes. Experiments to determine the achievable resolution of polysilane resists are in progress.

## **DISCLAIMER**

This report was prepared as an account of work sponsored by an agency of the United States Government. Neither the United States Government nor any agency thereof, nor any of their employees, makes any warranty, express or implied, or assumes any legal liability or responsibility for the accuracy, completeness, or usefulness of any information, apparatus, product, or process disclosed, or represents that its use would not infringe privately owned rights. Reference herein to any specific commercial product, process, or service by trade name, trademark, manufacturer, or otherwise does not necessarily constitute or imply its endorsement, recommendation, or favoring by the United States Government or any agency thereof. The views and opinions of authors expressed herein do not necessarily state or reflect those of the United States Government or any agency thereof.